Pharm Res (2015) 32:2704–2712
DOI 10.1007/s11095-015-1654-x

RESEARCH PAPER

A Microfluidic Diffusion Cell for Fast and Easy Percutaneous Absorption Assays

Christophe Provin • Alexandre Nicolas • Sébastien Grégoire • Teruo Fujii

Received: 18 December 2014 / Accepted: 10 February 2015 / Published online: 28 February 2015

ABSTRACT

Purpose Percutaneous absorption assays of molecules for pharmaceutical and cosmetology purposes are important to determine the bioavailability of new compounds, once topically applied. The current method of choice is to measure the rate of diffusion through excised human skin using a diffusion cell. This method however entails significant drawbacks such as scarce availability and poor reproducibility of the sample, low sampling rate, and tedious assay setup.

Methods The objective of the present work is to propose an alternative method that overcomes these issues by integrating an experimental model of the skin (artificial stratum corneum) and online optical sensors into a microfluidic device.

Results The measurement of the diffusion profile followed by the calculation of the permeability coefficients and time lag were performed on seven different molecules and obtained data positively fit with those available from literature on human skin penetration. The coating of the lipid mixture to generate the artificial stratum corneum also proved robust and reproducible. The results show that the proposed device is able to give fast, real-time, accurate, and reproducible data in a user-friendly manner, and can be produced at a large scale.

Conclusion These assets should help both the cosmetics and pharmaceutics fields where the skin is the target or a pathway of a formulated compound, by allowing more candidate molecules or formulations to be assessed during the various stages of their development.

KEY WORDS membrane · online monitoring · permeability coefficient · stratum corneum · time lag

ABBREVIATIONS

cv	Coefficient of variation
D	Coefficient of diffusion
K_p	Permeability coefficient
PAMPA	Parallelized artificial membranes penetration assay
PBS	Phosphate buffered saline
PDMS	Polydimethylsiloxane
SC	Stratum corneum
THJ	Tetra-hydro-jasmonic acid
t_{lag}	Time lag

INTRODUCTION

The total skin surface is about 1.7 m^2 for an average adult, and skin accounts for about 5.5% of the body weight (1). One of the main functions of the skin is to act as a barrier to an insensible loss of tissue water and to the penetration of exogenous molecules in the body. It is generally admitted (2)

Electronic supplementary material The online version of this article (doi:10.1007/s11095-015-1654-x) contains supplementary material, which is available to authorized users.

C. Provin (✉) • T. Fujii
LIMMS/CNRS-IIS (UMI 2820), Institute of Industrial Science
The University of Tokyo
4-6-1 Komaba, Meguro-ku 153-8505, Tokyo, Japan
e-mail: cprovin@iis.u-tokyo.ac.jp

T. Fujii
e-mail: tfujii@iis.u-tokyo.ac.jp

A. Nicolas
Nihon l'Oréal K.K., KSP R&D
3-2-1 Sakado, Takatsu-ku, Kawasaki-shi 213-0012, Kanagawa, Japan

S. Grégoire
L'Oréal Research and Innovation
1 avenue Eugène Schueller BP22, 93601 Aulnay s/s bois, France

Present Address:
C. Provin
Nikon and Essilor International Joint Research Center Co., Ltd. KSP R&D Build. C10F-1032 3-2-1, Sakado, Takatsu-ku, Kawasaki-shi
?213-0012, Kanagawa, Japan

that the main element that acts as a barrier is the outermost layer of the skin, the stratum corneum (SC). It is composed of 10 to 15 layers of flat keratinized cells (corneocytes) surrounded by a continuous lamellar lipid domain (3), the average thickness of which ranges 10–20 μm in most skin sites.

When developing new skin cosmetics or transdermal drug delivery systems, it is mandatory to get data on the percutaneous penetration of a compound to evaluate its bioavailability in order to assess its safety and efficiency. *In vivo* evaluation is often performed on human volunteers using tape stripping to peel-off the SC followed by analysis by liquid scintillation counting (4), HPLC or ATR-FTIR (5) for example. Such methods, however, are not satisfying as the subjects may be exposed to chemicals with unknown side effects or an excessive quantity. In addition, animal testing is banned in several parts of the world (for instance in EU (6)) for evaluating both ingredients and finished cosmetic products. Therefore *in silico* and *in vitro* evaluation of the skin bioavailability shall be preferred especially during the early phase of development of a new ingredient where final dosage and formulation are yet to be determined. *In silico* models are mainly based upon the pioneering work by Potts and Guy (7), which relies on an empirical equation relating permeant size/molecular weight and octanol/water partition coefficient (log P). Although convenient, the accuracy of such simple models is not very high (R^2=0.67). More complex models have been developed to address these shortcomings (8, 9) but they either need the input of extended experimental data that may not be available for newly developed compounds, or they are too complex to the non-expert, therefore limiting their appeal.

In vitro experiments are then the way of choice to get percutaneous absorption data during early stage of drug/cosmetic research. Two main approaches exist: systems derived from Parallelized Artificial Membranes Penetration Assay (PAMPA) (10) aiming at high Throughput Screening (HTS), and systems based on Franz cell (or diffusion cell) using natural skin or an artificial substrate as a diffusion membrane and suited for analysis of a single sample at a time. The first use of a PAMPA technique for evaluating at the skin barrier is rather recent (11) using a silicone/isopropyl myristate as a solvent in the receptor compartment. A more recent variant (12) involves the use of a membrane coated with a synthetic lipids mixture with a similar composition to that of skin SC. Although cost-effective, these methods still necessitate a sampling step and off-line quantitative analysis. Systems based on a Franz cell consists of a membrane sandwiched between a donor and a receptor compartments. The membrane can be either artificial such as silicone (13) or natural such as hairless mouse skin (14, 15) or excised human skin, often considered as the gold standard for penetration absorption studies by legislators. However, large variability intra and inter laboratories has been reported (16, 17) in addition to variability in the skin samples, whose availability remains difficult. The preparation of the sample and setting-up of the Franz cell system is time-consuming, and data acquisition rate is slow due to the necessity of repeated samplings. Therefore the percutaneous absorption assay using Franz cell with human skin is usually restricted to the final steps of product development.

As summarized by Whitesides (18), microfluidics is the science and technology of systems that handle minute amounts (10^{-9} to 10^{-18} L) of fluids, using channels of tens to hundreds of micrometers. They offer several advantages over conventional macroscopic systems such as a fast response due to the confined volume, miniaturization, integrated functionalities within the device (sensing, mixing, sampling, etc.) and automation, which led to successful applications in various fields such as analytical chemistry (19) or biology (20), but only recently did some applications specifically targeting the skin functionalities emerged (21). In this study, we propose to use the advantages of microfluidics to overcome the problems associated with percutaneous absorption assay using Franz cell through combining an artificial membrane designed to mimic the lipid composition of the SC with online absorption spectroscopy monitoring integrated in a microdevice. The technologies used to manufacture such device are simple enough to allow a scaling-up in their manufacture.

MATERIALS AND METHODS

Device Materials and Preparation

The device is made of 3 functional elements (Fig. 1): on top is a donor compartment where the sample is poured, in the middle is a membrane coated with lipids to act as an artificial SC, and at the bottom is a receptor and detector compartment.

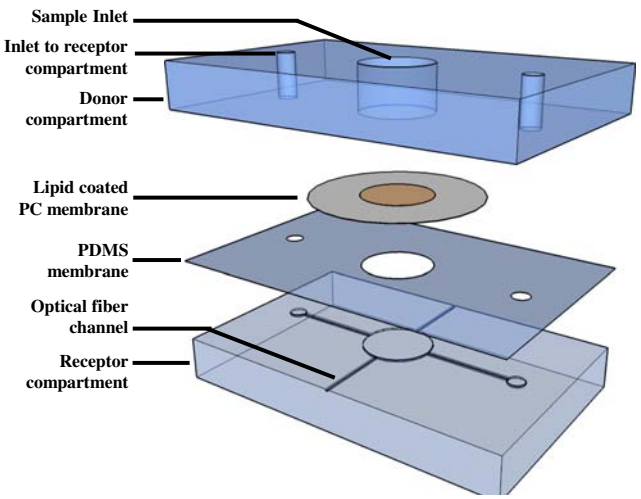

Fig. 1 Exploded schematic view of the complete device. Top layer: donor compartment with inlet for sample (diameter: 8 mm), and inlets/outlets (diameter: 1 mm) to fill the bottom layer. Middle layer: membrane coated with lipids to mimic the SC. Bottom layer: receptor compartment with fluidic channels to fill it, and channels separated from the main chamber by a 100 μm PDMS wall to insert the optical fibers for detection. The bottom layer is covered –except on top of the chamber and at the extremities of the filing channels- by a thin (~30 μm) PDMS membrane.

The donor compartment is made of a thick (~0.5 mm high) and flat piece of polydimethylsiloxane (PDMS, Silpot 184, Dow Corning, Japan). To prepare this part, PDMS liquid monomer and its curing agent are mixed at a 10:1 ratio, degassed and spread evenly, and then cured at 75°C for 1.5 h. The polymerized PDMS is then cut in pieces of about 2.5×4 cm, and subsequently holes for sample filler (diameter: 8 mm) and inlets connected to the receptor compartment (diameter: 1 mm) are drilled using a biopsy punch.

The receptor compartment consists of a central detection chamber (diameter: 8 mm) connected to the inlets from the donor compartment thanks to two 400 µm wide microchannels by two other channels (200 µm wide) dedicated to the insertion of the optical fibers are set across the chamber and are separated from it by a 100 µm wall. The preparation process of this compartment follows conventional soft lithography techniques (22). Briefly, the master mold is done with SU-8 2075 (Microchem, Japan) negative photoresist spin-coated on a silicon wafer to give a 200 µm thick layer. After UV irradiation through a chromium mask and solvent development, the resulting mold is coated with a CHF_3 layer thanks to a Reactive Ion Etching machine (RIE-10NR, Samco, Japan) in order to ease the demolding. Finally, a PDMS mix is poured over the SU-8 master mold and cured according to the same protocol as above. After demolding, the PDMS casting of the receptor compartment is covalently bonded to a PDMS membrane (~30 µm thick) using an O_2 plasma in the RIE machine to seal the fibers and fluidic channels in order to avoid leakage and to ease the bonding to the polycarbonate membrane. This PDMS membrane is obtained by spin-coat of a PDMS mix on a silicon wafer at 3000 rpm for 30 s followed by curing. Holes corresponding to the diameter of the chamber and the extremities of the fluidic channels are then cut out from the PDMS membrane to allow both the filling and the diffusion to take place in the receptor compartment (which final height is therefore 230 µm).

The central membrane (Nuclepore, Whatman, Japan) is made of a 19 mm diameter hydrophilic polycarbonate material comprising 50 nm pores. To increase the bonding quality between this membrane and the rest of the PDMS device, the membrane is soaked into a 5% solution of aminopropyltriethoxysilane for 1 h and then dried before use (23).

As a final step, the receptor compartment and the polycarbonate membrane are bonded together using an O_2 plasma in the RIE machine, and the resulting part is aligned and bonded to the donor compartment using the same procedure. A last oxygen plasma is used to bond the bottom of the whole device to a glass slide for an easy handling.

Lipid Coating Solution and Setup

One advantage of our microfluidic device for percutaneous absorption assay is the use of a lipid layer, the composition of which is rather close to a human SC (24). The lipid solution is composed of an equimolar mixture of fatty acids, cholesterol and ceramides dissolved at 7 g/L in a solvent composed of hexane and ethanol at 2:1 v/v, according to Bouwstra *et al.* (24, 25) This same group demonstrated that the lipid organization and barrier function of the *in vivo* SC were closely mimicked by the artificial SC. The lipid mixture is however slightly different since all the ceramides able to fully mimic the *in vivo* human SC composition are unavailable commercially. This difference could impact the structuration of the artificial SC (26), and increase the measured permeability (27). In addition, no thermal annealing was applied to the coated lipid unlike the recommendation by Groen *et al.* (25) to avoid mechanical stress in the device leading to possible leakage and to shorten the overall preparation time. The detailed lipid composition is given in Table S1.

The lipid solution is coated on the polycarbonate membrane sandwiched in the PDMS device by a micro spray valve 787MS-SS coupled with a 7140 controller (Nordson, Japan). The distance between the spray and the membrane is chosen to obtain a homogeneous sprayed area of about 1 cm in diameter. A spray cycle is as follows: the valve is open for 0.2 s, and then a waiting time of 8.8 s is used to let the surface dry. This cycle is looped for 600 times to reach the final deposited thickness. After letting the solvent evaporate completely overnight, the device is ready for use (Fig. 2). To determine the suitable thickness of lipids, preliminary diffusion experiments are carried out with various thicknesses to get a profile of diffusion compatible with previous reports within an acceptable preparation time. These experiments lead us to choose an arbitrary lipid thickness of 65 µm immediately after the end of the spray step, which corresponds to approximately 44 µm after drying overnight. The spray process is reproducible, giving a height h_{lip} of lipid measured at 44±13 µm after drying overnight (n=25, measured with a laser profilometer). This value is larger than the common thickness of SC, *i.e.,* around

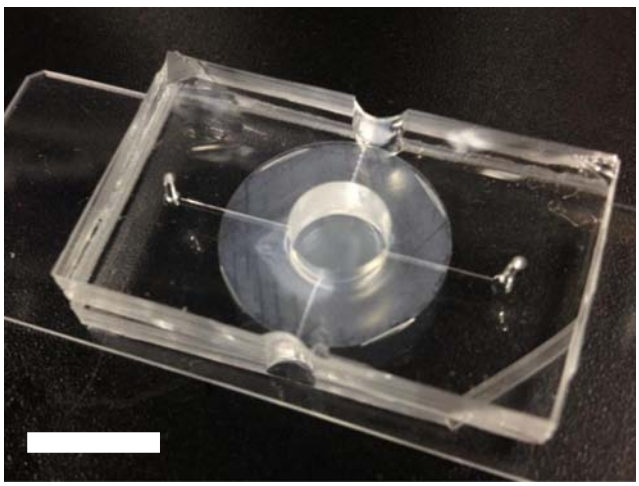

Fig. 2 Photograph of the final microdevice bonded on a glass slide. Scale bar is 1 cm.

10–20 μm, as it accommodates for the tortuosity of the continuous lipid phase which leads to a longer effective pathway to cross the skin barrier than its simple cross-section (28). To demonstrate the efficiency of the lipid coating, a control diffusion experiment with caffeine and fluorouracil through a bare polycarbonate membrane was performed and the resulting coefficients of diffusion (which will be defined in the next section) were respectively 15 and 25 times larger than with the lipid coating, and the resulting time lags (also defined in the next section) were inferior to 2 min for both compounds.

Molecules and Sample Preparation

Antipyrine (CAS Number: 60-80-0) is purchased from Fluka (Japan), 5-fluorouracil (CAS Number: 51-21-8) from TCI (Japan), aminopyrine (CAS Number: 58-15-1) and caffeine (CAS Number: 58-08-2) both from Wako (Japan). In addition cosmetic ingredients phenylethyl resorcinol (CAS Number: 85-27-8) is obtained from Symrise, and 4-butyl resorcinol (CAS Number: 18979-61-8) and tetra-hydro-jasmonic acid (THJ) (29) at a 32%wt concentration in water/dipropylene glycol (weight ratio of THJ:water:glycol is 32:48:20) are provided by L'Oréal Research (Aulnay s/s bois, France). Sample solutions are prepared by dissolving each compound is dissolved in Milli-Q water (Gradient A10, Millipore) at its respective saturation concentration C_{sat}, *i.e.,* 819 g/L for antipyrine, 17.1 g/L for fluorouracil, 55.9 g/L for aminopyrine, 20 g/L for caffeine, 2.5 g/L for phenylethyl resorcinol, 3.2 g/L for 4-butyl resorcinol, and THJ is used as received.

Detection Method

UV-visible absorption spectrometry is chosen since it is sensitive, compatible with an *in situ* detection method (connections with optical fibers), doesn't require any sample preparation (labeling or pre-concentration) and is easy to use and setup. To keep the overall set-up in a contained footprint, a USB2000+ miniature spectrophotometer from Ocean Optics (with UV gratings) is employed. The light source is a deep UV deuterium lamp (DH2000-S-DUV from Ocean Optics). Both the spectrophotometer and the lamp are connected to the device with a pair of high OH-content solarization-resistant optical fibers (Ocean Optics). A PC controls both the lamp shutter through a homemade interface and the spectrophotometer for parameters settings and data acquisition. The physical distance traveled by light through the studied medium is 8 mm, and the spectra obtained represent an average of 5 successive scans. Prior to the diffusion experiments, a mock-up device (*i.e.,* a device of which only the receptor compartment is used for this specific purpose) is used to determine the maximum absorption wavelength of the samples in the 200–300 nm range, and to establish their respective calibration curves. The latter are generally linear up to hundreds of ppm in general, and fitted with a first-order straight line with a zero intercept, yielding an average coefficient of determination $R^2 = 0.987$, proving that a quantitative analysis can be done with the presented system. The details of the calibration curves are shown in Table S2.

Diffusion Experiment

The device is positioned onto a digital hotplate (HP-1SA, AsOne), and a plastic case (with pass-through for the optical fibers) is set on top of the hotplate to keep a stable temperature of 32 ± 1°C, measured on top of the membrane using an infrared thermometer. The fibers for excitation and detection are inserted in the dedicated channels. A Dulbecco's Phosphate Buffered Saline 10X solution (Sigma) is diluted ten times in Milli-Q water. The resulting 1X PBS solution is warmed-up in a bain-marie (or water bath, at about 50°C) and degassed in a vacuum chamber for several minutes to avoid the formation of bubbles after injection. The volumes of donor and receptor fluids are calculated so their respective heights in the sample port and inlet/outlet ports are equal, in order to avoid pressure-driven flow and membrane deformation. Therefore 16.8 μL of the degassed PBS solution is slowly injected in the receptor compartment. The integration time of the spectrometer is then adjusted to maximize the signal at the wavelength of interest (typically 10–100 ms). Then, 126 μL of the saturated solution of the sample (for being at infinite-dose condition) is injected into the donor compartment, which is further covered with a piece of Parafilm® to limit evaporation. The plastic case is closed and the acquisition phase is started, with a rate of 1 data per 3 min (or 5 min for caffeine) to avoid saturation of the spectrometer by a continuous irradiation. For each sample, 4 to 5 devices are used to average the data.

RESULTS AND DISCUSSION

Diffusion Curve and Equation

Typically, the resulting curve of a diffusion experiment (with the cumulative permeated amount Q in the y-axis, and the time t in x-axis), is composed of 3 steps: a slow increase at the beginning (initial transient state) corresponding to the passage of the molecule through the membrane and the beginning of the diffusion, a steep linear increase corresponding to the steady state of the diffusion, and a slow increase at the end (final transient state) corresponding to the concentration in the receptor compartment becoming saturated. An example of curve obtained for the diffusion of caffeine in the presented microdevice is given in Fig. 3(a). This curve demonstrates that the sink conditions are respected in our experimental conditions. It is also the case for all tested molecules even those of the lowest water solubility.

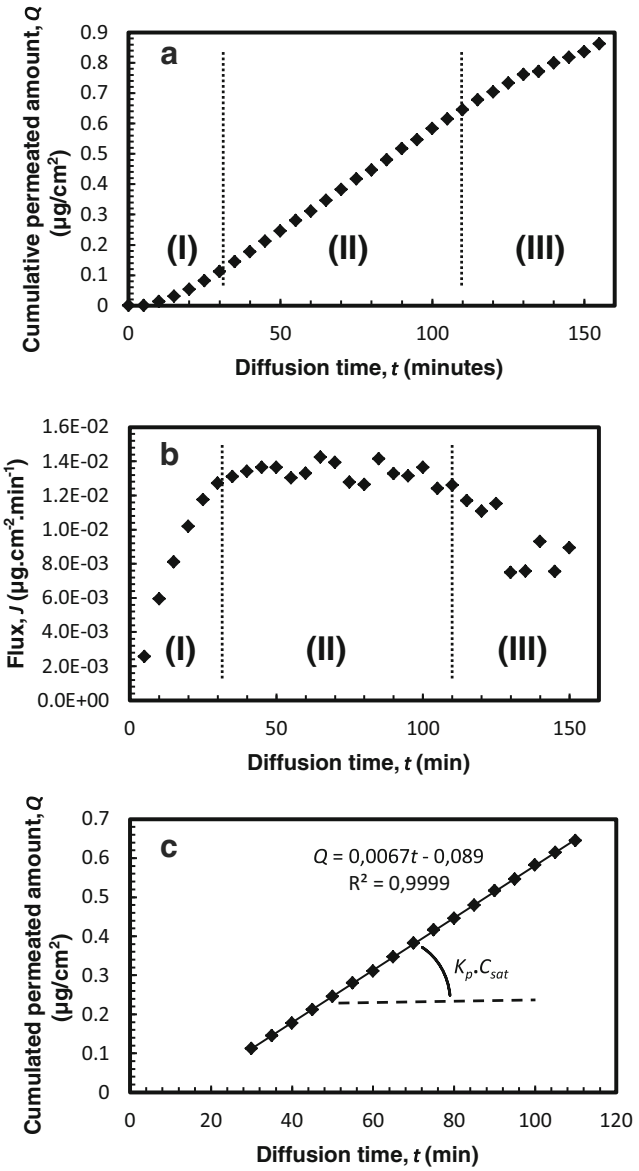

Fig. 3 Typical example of experimental data obtained with the presented device for the diffusion of caffeine. The various states of diffusion are separated by dashed lines and noted as I. Initial transient state. II. Steady state. III. Final transient state. (**a**) Experimental curve of the cumulated permeated amount *Q* as a function of the diffusion time *t*. (**b**) Derivative curve *dQ/dt* (equals to the flux *J*) of the data in Fig. 3a as a function of time *t*. In the steady state, the curve is flat. (**c**) Close-up on only the steady-state part of the curve in Fig. 3(a) (for the sake of readability). The regression line and its equation and coefficient of determination are written above. The slope of the regression line corresponds to the product of the permeability coefficient K_p by the concentration of the donor solution C_{sat}.

At steady state, the equation of diffusion is

$$Q_{ss} = K_p \cdot C_{sat} \cdot \left(t - t_{lag}\right) \tag{1}$$

With Q_{ss} the cumulative amount at the steady state, C_{sat} the concentration in the donor compartment, t the time and t_{lag} the lag time.

The derivative against time of Eq. 1 gives the maximum flux at steady state J_{ss}.

$$\frac{dQ_{ss}}{dt} = J_{ss} = K_p \cdot C_{sat} \tag{2}$$

Therefore K_p value is determined from the slope of the tangent to the experimental curves at steady state, and the lag time t_{lag} is determined by calculating the intercept of this tangent with the abscissa, and represents the time necessary to reach a stabilized concentration gradient across the membrane. Besides this information, t_{lag} may also be used to determine the coefficient of diffusion D in the artificial stratum corneum (30), using Eq. 3 (31).

$$D = \frac{{h_{lip}}^2}{6t_{lag}} \tag{3}$$

The online monitoring used in this study leads to a better defined experimental curve than with conventional Franz cells (32) or well inserts (33) which require a sampling step leading to an acquisition rate of 1 point per hour at best (*i.e.*, 20 times less defined). This high sampling rate greatly contributes to obtain quality results, *i.e.*, an accurate determination of the steady state part of the curve. The latter -theoretically linear, *i.e.*, of a constant derivative- (Fig. 3(b)) allows the permeability coefficient K_p and the lag time t_{lag} to being precisely measured, as shown in Fig. 3(c). In addition, the increased number of data shall make possible a rapid estimation of K_p from the very first data points of the steady state, affording a fast preliminary screening of candidate molecules.

Permeability Coefficient

The results are shown in Table I, comparing our data with those obtained with conventional methods using human epidermis. A robust model shall be able to qualitatively discriminate the diffusion of molecules of various physico-chemical properties, and gives values of K_p within a comparable range to those on real skin. For this purpose, the molecules chosen have a range of K_p values on human epidermis spanning two orders of magnitude (from 1.58×10^{-5} cm/h for fluorouracil to 5.01×10^{-3} cm/h for THJ), of various molecular weights and various hydrophobicity. The values of K_p obtained from our device show that the discrimination of such an array of molecules is possible, with a similar two orders of magnitude span (10^{-3}–10^{-5}). The inter variability between different devices (4 or above) is relatively acceptable with an averaged coefficient of variation (*cv*) of 52.3%, except for fluorouracil (*cv*: 75.8%), probably due to its very slow diffusion, making the results more prone to variation of the experimental conditions (humidity or external temperature during night). As regards the quantitative evaluation of the performance of the device, it

Table I Summary of Molecular Weight *MW*, Octanol/Water Partition Coefficient *P*, Concentration of the Solution at Saturation Used in the Donor Compartment, Wavelength of Maximal Absorption λ_{max}, K_p and t_{lag} from the Literature Obtained on Human Epidermis and by Calculation for the Set of Molecules Evaluated, Together with Experimental Values of K_p, t_{lag}, *D* with Standard Deviation ($n \geq 4$) Obtained on the Proposed Device

Molecule	*MW* (g/mol)	*Log P**	C_{sat} (g/L)	λ_{max} (nm)	K_p lit. (cm/h)	t_{lag} lit. (min)	Reference	K_p exp. (cm/h) $n \geq 4$	*cv* (%)	t_{lag} exp. (min)	*cv* (%)	*D exp.* (cm/h)
5-fluorouracil	130	−0.89[a]	17.1	269	1.58×10^{-5} 1.66×10^{-5} $(2.46 \pm 0.29) \times 10^{-5}$		Morimoto(32) Rigg(14) Williams(34)	$(1.90 \pm 1.44) \times 10^{-5}$	75.8	86 ± 44	51.2	6.25×10^{-10}
Antipyrine	188	0.38[a]	819	245	6.58×10^{-5}		Morimoto(32)	$(1.35 \pm 0.90) \times 10^{-5}$	66.7	21 ± 10	47.6	2.56×10^{-9}
4-butyl resorcinol	110	3.14[b]	3.2	282	2.40×10^{-4}	80	Roberts (35)	$(2.44 \pm 0.53) \times 10^{-4}$	21.7	91 ± 88	96.7	5.91×10^{-10}
Phenylethyl resorcinol	214	2.11[c]	2.5	281	3.7×10^{-4}		*In silico*	$(1.61 \pm 0.57) \times 10^{-4}$	35.4	184 ± 41	22.2	2.92×10^{-10}
Caffeine	194	−0.07[a]	20	273	7.6×10^{-5} $(9.36 \pm 0.83) \times 10^{-5}$ 3.85×10^{-4} 1.01×10^{-3} $(1.6 \pm 0.7) \times 10^{-3}$	105 ± 94 240 ± 108	Schreiber(36) Netzlaff(37) L'Oréal[b] Shäfer-Korting(38) Southwell(39)	$(2.33 \pm 1.13) \times 10^{-5}$	48.5	57 ± 31	54.4	9.43×10^{-10}
Aminopyrine	231	1[a]	55.9	247	1.02×10^{-3}		Morimoto(32)	$(1.18 \pm 0.70) \times 10^{-4}$	59.3	57 ± 23	40.3	9.43×10^{-10}
THJ	214	2.79[b]	320[d]	220	5.01×10^{-3}		*In silico*	$(2.22 \pm 1.30) \times 10^{-3}$	58.6	203 ± 112	55.2	2.65×10^{-10}

[a] From SRC Physical Properties Database

[b] Experimental value given by L'Oréal (personal communication)

[c] Calculated value using cLogP from Sybil Software

[d] Concentration in Water/Dipropylene Glycol mix (weight ratio of THJ:Water:Glycol is 32:48:20)

In silico: Value obtained using the equation $\text{Log } K_p = -2.71 + 0.71 \text{Log } P - 0.0061 MW$ from Potts & Guy (7)

is difficult to define a strict criterion to judge whether the measured K_p values are acceptable or not. Indeed, large variations occur in the experimental results on human skin in the literature (17), which are illustrated in Table I, such as caffeine (21-fold difference between lowest and highest figure). According to Chilcott (16), 35% variability is solely due to the difference in experimental conditions, but most significantly comes from differences in the skin samples since variations in the barrier function ranges from 2- to 6-fold between individuals and between anatomical sites (40). For this reason, another study pointed out the need to choose a consistent database obtained with a homogeneous protocol to compare one's experimental results (12). However, according to the molecules tested, such a database cannot be found. Therefore, in our case, a difference of several folds between the measured K_p and the values found in the literature can be considered as acceptable. The measured K_p are all in a good agreement with those from literature, with values ranging from being almost equals (0.83-fold lower) for fluorouracil up to 8-fold lower for aminopyrine. Actually, our experimental K_p are almost systematically lower than those reported on real skin or *in silico*. Since the lack of several types of ceramides in the used lipid composition has been correlated with an increase in the K_p value up to 2-fold (27), this is unexpected. It may suggest that the chosen lipid thickness is too high, or it may simply be a bias due to the lack of sufficient data to refer to.

A Concrete Application: The Case of THJ

THJ is a molecule derived from jasmonic acid that shows anti-aging properties (28). The water solubility of the neutral form being as low as 0.0055%wt (calculated with Episuite, WSKOW v1.41), it is often associated with dipropylene glycol to increase drastically its dissolved concentration. This association presents an issue for the *in silico* estimation of K_p using the Potts and Guy relation (7), as it is only valid in the case of aqueous solution. For this reason, it is a good example of a compound which diffusion can only be evaluated experimentally to determine its properties in practical conditions. In addition, the dipropylene glycol is a solvent often used in cosmetic formulations, and thus the evaluation of the THJ in a solution containing 20%wt is relevant to assess the robustness of the device and especially the lipid coating against a common non-aqueous vehicle. Another challenge presented by this molecule is its ability to be detected by UV absorption spectroscopy. Indeed THJ's only chromophores are a carbonyl and a cyclopentanone functions. This situation is representative of many actual cosmetic agents that don't possess strong absorbing chemical groups. Nonetheless, two absorption bands are found at 220 nm and 273 nm showing that the choice of a spectroscopy working in the deep-UV makes the proposed analytical method more versatile than could be primarily expected. The experimental K_p is 2.22×10^{-3} cm/h, which is the same order as the calculated value in water (5×10^{-3} cm/h, used as a rough benchmark). After the experiments, the coating didn't show any visible sign of degradation indicating that it is possible to use the device to test molecules dissolved in vehicles different from pure water.

Time Lag

The time lag value is seldom reported in the literature for two probable reasons. At first, the Flynn database (41), the first one that aggregated the percutaneous absorption data of 92 molecules and widely used to evaluate models, lacks such information. Second, the time lag value strongly depends upon the determination of the slope of the steady state (39) which usually suffers from a lack of experimental data points. The knowledge of the time lag is nonetheless crucial for transdermal drug delivery system, when its minimal value is looked for. As seen in Fig. 3(c), the slope can be determined with great confidence ($R^2=0.9999$) on a large number of data (16 experimental points), which is way better than conventional Franz cell assay where compromises have to be made between confidence and number of data with for example $R^2=0.8$ for 6 points or $R^2=0.9$ for 4 points for the determination of the steady state (38). Hence, amongst the molecules tested here, only time lag values for caffeine and 4-butyl resorcinol were found in the literature (Table I). Concerning 4-butyl resorcinol, the value we obtain (91 min) is in very good agreement with the work by Roberts *et al.* (35) which found 80 min. While on average the *cv* of time lag is 52.5% for the entire set of tested compounds, it is unusually high at 97% for 4-butyl resorcinol, reason of which remains unclear. For caffeine, the reported time lag varies from 105 min (38) to 240 min (39). In comparison, our recorded value of 57 min is shorter albeit of the same order. Using Eq. 3, and thanks to the controlled lipid thickness of the artificial SC, the coefficient of diffusion in the lipid coating can be easily determined and varies from 2.56×10^{-9} cm/h for antipyrine to 2.65×10^{-10} cm/h for THJ, which is in the order of estimated general values for such a coefficient (from 10^{-9} to10^{-12} cm/h) in the case of human skin (31, 42).

Microfluidics Contribution

Microfluidics is promising in several aspects. Besides the possibility to design an integrated system and the possibility to scale-up such devices, the small volume of the receptor compartment allows a fast responsive system since for a given flux and area of diffusion, the concentration is higher than in a macroscopic system. For the same reason, it makes it possible to rely only on passive diffusion (*i.e.*, without stirring) to obtain a homogeneous concentration in the receptor compartment. Indeed, the time for diffusion in one dimension follows $t_{diff}=l^2/2D_w$. Considering the height of the receptor chamber ($l=$

230 μm), and the diffusion coefficient in water ($D_w = 5 \times 10^{-6}$ cm^2/s), a rough estimation for caffeine leads to an approximate 52 s time to reach the bottom of the receptor compartment. Furthermore the dimensions of the receptor compartment are more biologically relevant than conventional Franz cells, the height of which is commonly in the order of the centimeter, whereas the thickness of epidermis is around 60–80 μm (43, 44) and that of total skin (epidermis plus dermis) ranges between 1.5 and 2.5 mm (45). An interesting topic to discuss is the choice of PDMS as the base material for the device. Indeed, it is a common and convenient material for microfluidic device development, but it is also known that small hydrophobic molecules can be absorbed into its matrix (46) and affect the outcome of diffusion experiment. While this phenomenon may be of concern for several tested molecules, we didn't notice its influence on our results. First, in our experimental configuration the donor compartment can be considered as an infinite reservoir, preventing any significant variation of its concentration by absorption into the PDMS. Second, the surface/volume ratio of the receptor compartment is an order smaller than for the microchannels used by Toepke *et al.* (46), limiting the transfer of tested compounds into the PDMS walls. Last, we didn't notice any variation of the signal during the establishment of the calibration curves for UV absorption spectroscopy, indicating that a noticeable effect on the absorption reading is only likely to happen on a rather long time scale. In addition, the goal of this study is to demonstrate the potentiality of an integrated microfluidic device in the field of percutaneous absorption, therefore in the case of mass-production, PDMS is likely to be replaced by cheaper alternative polymers such as polymethyl methacrylate or polycarbonate whose diffusive properties are negligible in comparison.

CONCLUSIONS

The proposed microfluidic diffusion cell with biomimetic dimensions makes discriminating molecules possible, despite their various physico-chemical properties, and leads to experimental values of K_p and time lag in a close range to those from literature obtained on human skin biopsies with conventional Franz cell. The inter device variability is also acceptable, generally better than those reported for human epidermis biopsies and/or reconstructed epidermis. Furthermore, the choice of online detection allows a high data acquisition rate to be obtained without perturbing the system with sampling, leading to a higher quality of information since experimental curves are better defined, and steady state is more accurately defined. While not as sophisticated as liquid chromatography-mass spectrometry (the analytical method of choice for percutaneous absorption assay using Franz cell), UV absorption spectroscopy is several order of magnitude cheaper and less voluminous, allowing several systems to be run in parallel. Moreover other type of online monitoring analytical systems such as fluorescence (47) can be integrated in the microfluidic device to further expand the spectrum of detectable molecules.

ACKNOWLEDGMENTS AND DISCLOSURES

This collaborative work has been initiated in the frame of LIMMS/CNRS-IIS (UMI 2820), an international joint research laboratory between CNRS, France and IIS, University of Tokyo, Japan, and was supported by a grant from Nihon L'Oréal K.K. A patent application about the presented device (PCT/FR2013/051080) has been filed on May 16, 2013, with the authors listed as inventors. The authors would like to thank Dr. Haruyuki Kinoshita (IIS, The University of Tokyo) for measuring the lipid thickness and his help with the fabrication of devices, and Dr. Momoko Kumemura (LIMMS/IIS, The University of Tokyo) for her help with the fabrication of devices.

REFERENCES

1. Goldsmith LA. My organ is bigger than your organ. Arch Dermatol. 1990;126:301–2.
2. Scheuplein RJ. In Pollock DM, editor. Comprehensive Physiology, editor. Wiley; 2011. p. 299–322.
3. Elias PM, Brown BE, Fritsch P, Goerke J, Gray GM, White RJ. Localization and composition of lipids in neonatal mouse stratum granulosum and stratum corneum. J Invest Dermatol. 1979;73:339–48.
4. Rougier A, Dupuis D, Lotte C, Roguet R, Schaefer H. In vivo correlation between stratum corneum reservoir function and percutaneous absorption. J Invest Dermatol. 1983;81:275–8.
5. Pirot F, Kalia YN, Stinchcomb AL, Keating G, Bunge A, Guy RH. Characterization of the permeability barrier of human skin in vivo. Proc Natl Acad Sci U S A. 1997;94(4):1562–7.
6. Regulation (EC) No 1223/2009 of the European Parliament and of the Council of 30 November 2009 on cosmetic products (Text with EEA relevance), OJ L 342, 22.12.2009, p 59–209.
7. Potts RO, Guy RH. Predicting skin permeability. Pharm Res. 1992;9(5):663–9.
8. Moss GP, Wilkinson SC, Sun Y. Mathematical modelling of percutaneous absorption. Curr Opin Colloid Interface Sci. 2012;17(3):166–72.
9. Anissimov YG, Jepps OG, Dancik Y, Roberts MS. Mathematical and pharmacokinetic modelling of epidermal and dermal transport processes. Adv Drug Deliv Rev. 2013;65(2):169–90.
10. Faller B. Artificial membrane assays to assess permeability. Curr Drug Metab. 2008;9(9):886–92.
11. Ottaviani G, Martel S, Carrupt P-A. Parallel artificial membrane permeability assay: a new membrane for the fast prediction of passive human skin permeability. J Med Chem. 2006;49(13):3948–54.
12. Sinkó B *et al.* Skin–PAMPA: a new method for fast prediction of skin penetration. Eur J Pharm Sci. 2012;45(5):698–707.
13. Dias M *et al.* Topical delivery of caffeine from some commercial formulations. Inter J Pharm. 1999;182(1):41–7.

14. Rigg PC, Barry BW. Shed snake skin and hairless mouse skin as model membranes for human skin during permeation studies. J Invest Dermatol. 1990;94(2):235–40.
15. Bond JR, Barry BW. Limitations of hairless mouse skin as a model for in vitro permeation studies through human skin: hydration damage. J Invest Dermatol. 1988;90(4):486–9.
16. Chilcott RP *et al.* Inter- and intralaboratory variation of in vitro diffusion cell measurements: an international multicenter study using quasi-standardized methods and materials. J Pharm Sci. 2005;94(3): 632–8.
17. Van de Sandt JJM *et al.* In vitro predictions of skin absorption of caffeine, testosterone, and benzoic acid: a multi-centre comparison study. Regul Toxicol Pharm. 2004;39(3):271–81.
18. Whitesides GM. The origins and the future of microfluidics. Nature. 2006;442(7101):368–73.
19. Ohno KI, Tachikawa K, Manz A. Microfluidics: applications for analytical purposes in chemistry and biochemistry. Electrophoresis. 2008;29(22):4443–53.
20. Bhatia SN, Ingber DE. Microfluidic organs-on-chips. Nat Biotechnol. 2014;32(8):760–72.
21. Hou L, Hagen J, Wang X, Papautsky I, Naik R, Kelley-Loughnane N, *et al.* Artificial microfluidic skin for in vitro perspiration simulation and testing. Lab Chip. 2013;13(10):1868–75.
22. Xia Y, Whitesides GM. Soft lithography. Angew Chem Int Edit. 1998;37:550–75.
23. Sunkara V *et al.* Simple room temperature bonding of thermoplastics and poly(dimethylsiloxane). Lab Chip. 2011;11(5):962–5.
24. De Jager MW, Gooris G, Ponec M, Bouwstra J. Lipid mixtures prepared with well-defined synthetic ceramides closely mimic the unique stratum corneum lipid phase behavior. J Lipid Res. 2005;46(12):2649–56.
25. Groen D, Gooris G, Ponec M, Bouwstra J. Two new methods for preparing a unique stratum corneum substitute. Biochim Biophys Acta-Biomembranes. 2008;1778(10):2421–9.
26. Kessner D *et al.* Arrangement of ceramide [EOS] in a stratum corneum lipid model matrix: new aspects revealed by neutron diffraction studies. Eur Biophys J. 2008;37(6):989–99.
27. De Jager MW *et al.* A novel in vitro percutaneous penetration model: evaluation of barrier properties with P-aminobenzoic acid and two of its derivatives. Pharm Res. 2006;23(5):951–60.
28. Talreja PS, Kasting GB, Kleene NK, Pickens WL, Wang TF. Visualization of the lipid barrier and measurement of lipid pathlength in human stratum corneum. Aaps Pharmscitech. 2001;3(2):48–56.
29. Michelet JF *et al.* The anti-ageing potential of a new jasmonic acid derivative (LR2412): in vitro evaluation using reconstructed epidermis episkin™. Exp Dermatol. 2012;21(5):398–400.
30. Frisch HL. The time lag in diffusion. J Phys Chem. 1957;61(1):93–5.
31. Flynn GL, Stewart B. Percutaneous drug penetration: choosing candidates for transdermal development. Drug Develop Res. 1988;13(2): 169–85.
32. Morimoto Y, Hatanaka T, Sugibayashi K, Omiya H. Prediction of skin permeability of drugs - comparison of human and hairless rat skin. J Pharm Pharmacol. 1992;44(8):634–9.
33. Garrigues-Mazert A, Grégoire S, Zeman N, Meunier JR. A Pertinent screening tool to measure permeability coefficient : Episkin® Reconstructed Human Skin Model", 8th World Congress on Alternatives and Animal Use in the Life Sciences, 2011, Montreal, Canada.
34. Williams AC, Barry BW. Terpenes and the lipid–protein–partitioning theory of skin penetration enhancement. Pharm Res. 1991;8(1):17–24.
35. Roberts MS, Anderson RA, Swarbrick J. Permeability of human epidermis to phenolic compounds. J Pharm Pharmacol. 1977;29(1): 677–83.
36. Schreiber S *et al.* Reconstructed epidermis versus human and animal skin in skin absorption studies. Toxicol in Vitro. 2005;19(6):813–22.
37. Netzlaff F *et al.* Permeability of the reconstructed human epidermis model Episkin® in comparison to various human skin preparations. Eur J Pharm Biopharm. 2007;66(1):127–34.
38. Schäfer-Korting M. The use of reconstructed human epidermis for skin absorption testing: results of the validation study. Altern Lab Anim: ATLA. 2008;36(2):161–87.
39. Southwell D, Barry BW, Woodford R. Variations in permeability of human skin within and between specimens. Int J Pharm. 1984;18(3): 299–309.
40. Schaefer H, Redelmeier TE. Skin barrier, principles of percutaneous absorption. Basel: Karger; 1996. p. 310.
41. Flynn GL. Physicochemical determinants of skin absorption. In: Gerrity TR, Henry CJ, editors. Principles of route to route extrapolation for risk assessment. New York: Elsevier; 1990. p. 93–127.
42. Scheuplein KJ, Bronaugh RL. Percutaneous absorption. In: Goldsmith LA, editor. Biochemistry and physiology of the skin. New York: Oxford University Press; 1983, vol. 11, p. 1255–1295.
43. Sandby-Moller J, Poulsen T, Wulf HC. Epidermal thickness at different body sites: relationship to age, gender, pigmentation, blood content, skin type and smoking habits. Acta Derm Venerol. 2003;83(6):410–3.
44. Rees JL, Robertson K. Variation in epidermal morphology in human skin at different body sites as measured by reflectance confocal microscopy. Acta Derm Venerol. 2010;90(4):368–73.
45. Laurent A *et al.* Echographic measurement of skin thickness in adults by high frequency ultrasound to assess the appropriate microneedle length for intradermal delivery of vaccines. Vaccine. 2007;25(34): 6423–30.
46. Toepke MW, Beebe DJ. PDMS absorption of small molecules and consequences in microfluidic applications. Lab Chip. 2006;6: 1484–6.
47. Kimura H, Yamamoto T, Sakai H, Sakai Y, Fujii T. An integrated microfluidic system for long-term perfusion culture and on-line monitoring of intestinal tissue models. Lab Chip. 2008;8(5):741–6.